Submitted to The Astrophysical Journal
Preprint typeset using LaTeX style emulateapj v. 12/16/11

# METALS ON THE BH EXPRESS: OXYGEN TRANSPORT IN THE CGM OF SIMULATED MW-MASS GALAXIES

N. Nicole Sanchez[1], Jess Werk[1], Michael Tremmel[2], Andrew Pontzen[3], Charlotte Christensen[4], Tom Quinn[1], and Akaxia Cruz[1]

[1]Astronomy Department, University of Washington, Seattle, WA 98195, US, sanchenn@uw.edu
[2]Yale Center for Astronomy & Astrophysics, Physics Department, P.O. Box 208120, New Haven, CT 06520, USA
[3]Department of Physics & Astronomy, University College London, 132 Hampstead Road, London, NWI 2PS, United Kingdom and
[4]Physics Department, Grinnell College, 1116 Eighth Ave., Grinnell, IA 50112, United States

*Submitted to The Astrophysical Journal*

## ABSTRACT

**[UNDER CONSTRUCTION]** We examine the cosmological hydrodynamic simulation ROMULUS25 (Tremmel et al. 2017) and a suite of zoom-in "genetically modified" Milky Way-mass galaxies to study the effects of galaxy evolution and SMBH feedback on the CGM. We compare the column densities of OVI in the Milky Way-mass galaxies of ROMULUS25 and compare them with observations from the COS-Halos Survey. We determine that a galaxy's morphology has little effect on the appearance of OVI in its CGM while column densities of OVI are more likely tied to galaxy halo mass. The suite of zoom-in Milky Way-mass galaxies further confirm this result and further examine the effect of AGN feedback on the CGM's OVI. We find that SMBH feedback prescriptions act as the physical mechanism transporting metals out into its host halo thereby significantly impacting the appearance of OVI found in the CGM.

*Subject headings:* Gas physics – Galaxies: circumgalactic medium – Galaxies: spiral – Galaxies: kinematics and dynamics – Methods: Numerical

## 1. INTRODUCTION

The circumgalactic medium (CGM), the extended region of gas surrounding galaxies out to their virial radii, is a rich and vast yet mostly unexplored area of astronomy due to its diffuse, difficult-to-observe nature. Recent observations, due to technological advances like the Cosmic Origins Spectrograph (COS) on the HST, have allowed researchers to finally begin characterizing this mysterious component of all galaxies and find it to be a structurally complex, multiphase medium. (Werk 2012, 2013, 2014, Tumlinson 2011, Also cite Review + others) Examinations like Ford (Ford 2013) which showed that most of the "missing baryons" of galaxies likely resides in this diffuse region imply that the CGM may play a key role in the growth of galaxies and the build up of their disks. Therefore, it is clear that understanding the CGM is a significant component to understanding the complex nature of galaxy evolution and growth.

Several studies have been done to examine the effect of galaxy evolution on the CGM. Tumlinson 2011's COS-Halo observations show a correlation between the column densities of OVI and the specific SFR of their observed galaxy CGMs with higher abundances of OVI around SF galaxies compared to their passive counter parts. Subsequent arguments have been made to understand this result. Oppenheimer 2016 argue that this bimodality arises due to the OVI acting as a proxy for the virial masses of these galaxy halos, as the oxygen in the star forming galaxies are subsequently in the correct virial temperature range to maximize OVI production. Therefore, the more massive galaxies in the COS-Halo sample show less OVI in their CGM due to the intrinsically higher virial temperature of these massive red ellipticals. Other arguments have been made to explain this correlation however, as Suresh 2017 argues that the NOVI abundances in SF galaxies arise due to feedback from the AGN, which can physically sculpt via outflows or heat the CGM to appropriate temperature for ionizing OVI. In both cases, we see the argument for an intrinsic link between the CGM and its host galaxy's evolution.

Since galaxy evolution has been shown to be strongly tied to the evolution of its central supermassive black hole (SMBH) —through relations like the M-$\sigma$ and the bulge mass-BH mass correlation which indicates that the SMBH and its host galaxy halo *grow together* (Reines 2015, other from "Gebhardt et al. 2000a; Ferrarese & Merritt 2000; Marconi & Hunt 2003; Haring & Rix 2004; Gultekin et al. 2009; McConnell & Ma 2013; Kormendy & Ho 2013, and references therein" from Reines 2015) —it is unsurprising that the AGN is thought to also leave its marks on the CGM. However, the direct mechanisms by which the AGN impacts the CGM most readily are still hotly debated.

AGN are thought to effect the CGM in a number of ways. Feedback from the active SMBH may inject energy into the surrounding material, raising temperatures, and ionizing metals in the gas [**CITE**]. Outflows of gas from the AGN may also physically push gas out of the galaxy (some of which may end up falling back into the galaxy as part of the "recycling" of the CGM [**CITE; CGM review**]), enriching CGM gas with metals from the center of the galaxy, and furthermore enriching the IGM as gas is expelled from the galaxy. Since observations are limited to spectroscopic analysis (which can help us understand the abundances and structure of ions in the CGM), simulations are necessary to examine the physics driving the multiphase nature of the CGM.

Simulators have long been examining the underlying physics of AGN activity in galaxies; however, examining these effects in the diffuse region of the

CGM is still a fairly new expedition. We continue this trek of new discovery utilizing a cutting-edge suite of simulations: the cosmological volume, ROMULUS25 (Tremmel et al. 2017) and a single isolated, zoom-in Milky-Way (MW) mass galaxy (Roth et al. 2016; Pontzen et al. 2017) with three genetic modifications with and without the implementation of advanced BH physics (Tremmel et al. 2015). With these simulations, we plan to examine two specific questions with our study.

- How does the evolution of the galaxy imprint itself on the CGM?
- How does the AGN's activity imprint itself on the CGM?

Both the ROMULUS25 simulation and our suite of high-resolution, zoom-in simulations with genetic modifications will allow us to study the first question in detail as we examine the CGM in a range of MW-mass galaxies with varied morphologies. Additionally, from our isolated MW galaxy, h243, and its genetic modifications, we can examine the effect of AGN feedback on the CGM in a suite of galaxies run both with and without BH physics. Using these isolated, zoom-in simulations in tandem with the Romulus25 simulation, we hope to better understand the roles that galactic evolution and AGN feedback play in characterizing where OVI lives within the CGM of MW-mass galaxies.

## 2. SIMULATION PARAMETERS

### 2.1. *ChaNGa Physics*

Both ROMULUS25 (hereafter R25) and our suite of zoom-in galaxies were run using the smoothed particle hydrodynamics (SPH) N-body tree code, Charm N-body GrAvity solver [ChaNGa](Menon et al. 2015). ChaNGa includes the same models for a cosmic UV background, star formation, 'blastwave' SN feedback, and low temperature metal line cooling as previously used in GASOLINE (Wadsley et al. 2004, 2008; Stinson et al. 2006; Shen et al. 2010). ChaNGa includes an improved SPH formalism which includes a geometric density approach in the force expression: $(P_i + P_j)/(\rho_i \rho_j)$ instead of $P_i/\rho_i^2$ + $P_j/\rho_j^2$ where $P_i$ and $\rho_i$ are the particle's pressure and density, respectively. This update to the hydrodynamic treatment includes thermal diffusion (Shen et al. 2010) and reduces artificial surface tension allowing for better resolution of fluid instabilities (Ritchie & Thomas 2001; Menon et al. 2015; Governato et al. 2015). Additional improvements have been made to the BH formation, accretion, and feedback models as well an improved prescription for dynamical friction (Tremmel et al. 2015, 2017).

R25 and our suite of zoom-in galaxies were run with an ΛCDM cosmology from the most recent Planck collaboration utilizing $\sigma_0 = 0.3086$, $\alpha = 0.6914$, h = 0.67, $\sigma_8 = 0.77$ and have Plummer equivalent force softening lengths of 250 pc. For simulating the cosmic reionization energy, both simulations enact a UV background at z 9 using the formula of Haardt & Madau (2012). Some recent papers **[CITE]** have raised concerns that this UV background is too strong **[CITE]**. However, since our primary concern is the abundance of OVI which is considered to be collisionally ionized rather than photoionized **[CITE]**, our choice of UV background should not affect our results.

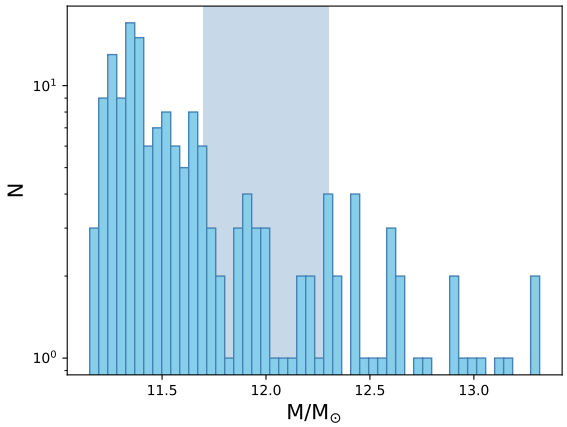


FIG. 1.— R25 is an SPH simulated cosmological volume with galaxies spanning the orders of $10^8$ —$10^{13}$ $M_\odot$. For clarity, we've plotted a histogram of only the galaxies in the volume with masses between $2 \times 10^{11}$ $M_\odot$ —$2 \times 10^{13}$ $M_\odot$ (The latter is the upper limit of galaxy masses in the volume.) The shaded region indicates the "MW" mass range, $5 \times 10^{11}$ $M_\odot$ —$2 \times 10^{12}$ $M_\odot$, from which we select our 26 galaxies.

### 2.2. *Romulus 25 Cosmological Volume*

The ROMULUS25 (Tremmel et al. 2017) simulation is a cosmological volume which includes galaxies within the mass range $10^8$ —$10^{13}$ $M_\odot$. R25 has a mass resolution of $3.4 \times 10^5$ $M_\odot$ and $2.1 \times 10^5$ $M_\odot$ for DM and gas particles, respectively. For our study, we focus on galaxies within the MW-mass regime, $5 \times 10^{11}$ $M_\odot$ —$2 \times 10^{12}$ $M_\odot$ (Figure 1). We examine all the galaxies within the specified mass range and exclude any galaxies within twice the virial of another galaxy, thereby removing galaxies that might be satellites of a larger galaxy. With these selection criteria in place, our sample includes 26 galaxies.

### 2.3. *h243 and its Genetically Modified Galaxies*

For our suite of genetically modified galaxies (GMs), an initial uniform-volume, 50 $h^{-1}$ Mpc on a side, DM-only cosmological volume was simulated. From this volume a MW-mass halo at z=0, h243, was selected as our "Patient 0" and re-simulated at a higher resolution. Patient 0 and its subsequent GM simulations have mass resolutions of $1.4 \times 10^5$ $M_\odot$ and $2.1 \times 10^5$ $M_\odot$ for DM and gas particles, respectively. The DM field in these galaxies is simulated at twice the gas linear resolution to reduce noise in the potential near the galactic center (Pontzen et al. 2017) and more accurately trace black hole dynamics (Tremmel et al. 2015).

#### 2.3.1. *Galaxies with BH Physics*

At z = 0, our "Patient 0" (hereafter P0) of the galaxy simulation h243 is a star forming galaxy with a disk and has a final main halo mass of $1.08 \times 10^{12}$ $M_\odot$ and virial radius ($R_{vir}$) of 269 kpc. It has total gas and stellar masses of $1.09 \times 10^{11}$ $M_\odot$ and $5.71 \times 10^{10}$ $M_\odot$, respectively (Table 1). Patient zero has an incoming satellite at z = 1 with an original mass of $7.34 \times 10^{10}$ $M_\odot$ (q = 0.12). For each GM galaxy simulation, we systematically

TABLE 1
GM Galaxies with BHs Simulation Details

| Sim | Total Halo Mass ($M_\odot$) | Total Gas Mass ($M_\odot$) | Total Stellar Mass ($M_\odot$) | CGM Gas Mass ($M_\odot$) | $R_{vir}$ (kpc) | $T_{vir}$ (K) | **Satellite Mass ($M_\odot$)** |
|---|---|---|---|---|---|---|---|
| P0 | $1.08 \times 10^{12}$ | $1.09 \times 10^{11}$ | $5.71 \times 10^{10}$ | $1.02 \times 10^{11}$ | 268.9 | $5.12 \times 10^{5}$ | **$7.34 \times 10^{10}$** |
| GM1 | $1.07 \times 10^{12}$ | $1.01 \times 10^{11}$ | $6.43 \times 10^{10}$ | $9.18 \times 10^{10}$ | 269.2 | $5.12 \times 10^{5}$ | **$5.86 \times 10^{10}$** |
| GM2 | $8.69 \times 10^{11}$ | $7.41 \times 10^{10}$ | $1.38 \times 10^{10}$ | X $\times 10^{10}$ | 254.1 | X $\times 10^{5}$ | **$3.97 \times 10^{10}$** |
| GM3 | $7.76 \times 10^{11}$ | $6.36 \times 10^{10}$ | $1.04 \times 10^{10}$ | $6.35 \times 10^{10}$ | 241.7 | $4.14 \times 10^{5}$ | **$2.45 \times 10^{10}$** |

shrink this satellite halo's mass prior to its merger with the main halo.

*GM1:* For our first GM galaxy, we shrink the satellite halo's mass to 5.86 $\times$ $10^{10}$ $M_\odot$ (q = 0.10). At z = 0, GM1 is a star forming galaxy with a disk and has a final halo mass of 1.07 $\times$ $10^{12}$ and $R_{vir}$ = 269 kpc. It has total gas and stellar masses of 1.01 $\times$ $10^{11}$ $M_\odot$ and 6.43 $\times$ $10^{10}$ $M_\odot$, respectively.

*GM2:* Our second GM galaxy has a incoming satellite mass shrunk to 3.97 $\times$ $10^{10}$ $M_\odot$ (q = 0.06). At z = 0, GM2 has a final halo mass of 8.69 $\times$ $10^{11}$ $M_\odot$ and $R_{vir}$ = 254 kpc. It has total gas and stellar masses of 7.41 $\times$ $10^{10}$ $M_\odot$ and 1.38 $\times$ $10^{10}$ $M_\odot$, respectively.

*GM3:* The third and final GM galaxy has a incoming satellite mass shrunk to 2.45 $\times$ $10^{10}$ $M_\odot$ (q = 0.04). At z = 0, GM3 has a final halo mass of 7.76 $\times$ $10^{11}$ $M_\odot$ and $R_{vir}$ = 242 kpc. It has a total gas and stellar masses of 6.36 $\times$ $10^{10}$ $M_\odot$ and 1.04 $\times$ $10^{10}$ $M_\odot$, respectively.

As these galaxies are all slight modifications of each other (but result in galaxies with different morphologies), these four "zoom-in" galaxy simulations allow us to directly examine the effect of morphology on the CGM.

#### 2.3.2. *Galaxies without BH Physics*

To isolate the effect of the AGN on the CGM, all four of the zoom-in simulations (P0 and its 3 GMs) were re-simulated at the same resolution and with all the same physics *excluding* BH formation, feedback, and dynamical friction (Table 2).

## 3. SIMULATION ANALYSIS

Individual halos in the ROMULUS25 cosmological volume and in the individual zoom-in galaxies are extracted using the Amiga Halo Finder (AHF) (Knollmann & Knebe 2009) and central SMBH positions and velocities are defined relative to the center position and inner 1 kpc center-of-mass velocity of their host halo, respectively. From R25, we specifically examine Milky Way-mass halos which are defined as halos between 5 $\times$ $10^{11}$ and 2 $\times$ $10^{12}$ $M_\odot$ and are at least twice a virial radii from their nearest neighbor (to exclude any satellites). All zoom-in galaxies are isolated with a minor merger at z=0.

The CGM of each individual galaxy halo (within the R25 galaxies and our zoom-ins) is defined as the mass enclosed from 10 kpc from the center position out to a virial radius defined as the radius at which 200 times the critical density, $\rho_c$, where $\rho/\rho_c$ = 200. Figure 3 shows the CGM of the 4 zoom-in galaxies with and without BH physics. Between the galaxies that exclude BH physics, the phase diagrams of the CGM do not vary significantly. There is also little difference between the phase diagrams of the CGM for the two star forming galaxies, P0 and GM1, in the case with or without BHs. The most noticeable change come between the star forming galaxies, P0 and GM1, with BH physics and those that are quenched, GM2 and GM3. There is more high temperature, high density gas in both P0 and GM1 than either GM2 or GM3. This difference likely stems from the continued star formation in P0 and GM1 which can heat the denser gas in the CGM which resides closest to the disk. **Check this description with Jess.** However, this difference doesn't seem to play a significant effect on the OVI that we see in the galaxies.

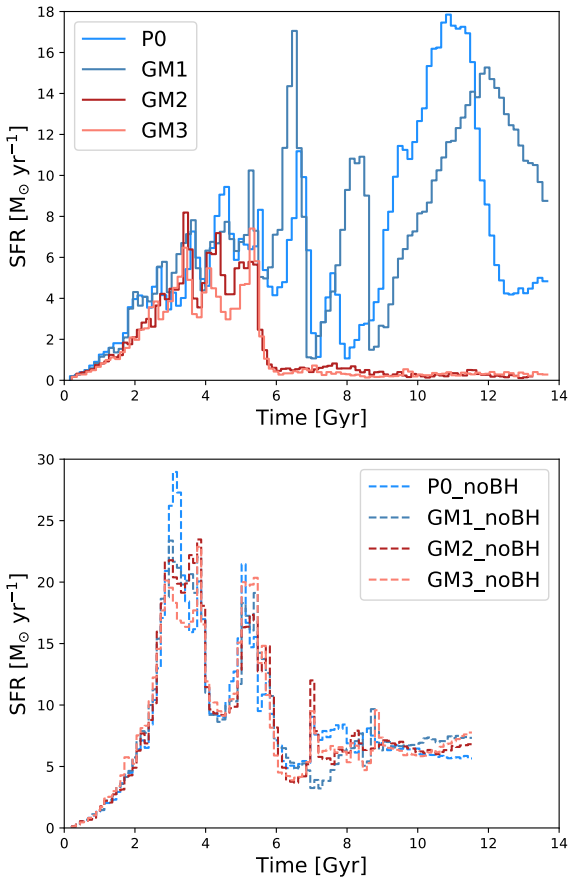


FIG. 2.— The star formation histories for the zoom-in galaxies: Patient 0 and its 3 GM galaxies with BH physics (*Upper*) and *Lower* without BH physics. In the galaxies including BH physics, P0 and GM1 remain star forming throughout their histories while GM2 and GM3 become quenched at z $\sim$ 1. Without BH physics, all four galaxies remain star forming until z = 0.

Column densities of OVI are calculated using the analysis software Pynbody [**PONTZEN 2013**]. Oxygen is traced throughout the time of the simulation and OVI ion fractions are calculated using a CLOUDY model [**Hennawi, Prockaska, Stinson**]. Figure 4 shows the column densities of OVI as a function of radius for our 26 R25 MW-mass galaxies. Red and blue lines describe

TABLE 2
Zoom-In Galaxies with NO BHs Simulation Details (AT z = 0.17)

| Sim | Total Halo Mass ($M_\odot$) | Total Gas Mass ($M_\odot$) | Total Stellar Mass ($M_\odot$) | CGM Gas Mass ($M_\odot$) | $R_{vir}$ (kpc) | $T_{vir}$ (K) | **Satellite Mass ($M_\odot$)** |
|---|---|---|---|---|---|---|---|
| P0 noBH | $8.36 \times 10^{11}$ | $7.0 \times 10^{10}$ | $7.37 \times 10^{10}$ | X $\times 10^{10}$ | 262.8 | X $\times 10^{5}$ | $\mathbf{7.34 \times 10^{10}}$ |
| GM1 noBH | $8.38 \times 10^{11}$ | $7.07 \times 10^{10}$ | $7.34 \times 10^{10}$ | X $\times 10^{10}$ | 263.0 | X $\times 10^{5}$ | $\mathbf{5.86 \times 10^{10}}$ |
| GM2 noBH | $8.42 \times 10^{11}$ | $7.08 \times 10^{10}$ | $7.33 \times 10^{10}$ | X $\times 10^{10}$ | 263.4 | X $\times 10^{5}$ | $\mathbf{3.97 \times 10^{10}}$ |
| GM3 noBH | $8.43 \times 10^{11}$ | $7.19 \times 10^{10}$ | $7.28 \times 10^{10}$ | X $\times 10^{10}$ | 263.5 | X $\times 10^{5}$ | $\mathbf{2.45 \times 10^{10}}$ |

quenched and star forming galaxies within the sample, respectively. The COS-Halo Survey dataset is plotted on top in black, with squares and circles distinguishing between elliptical and spiral galaxies. Upper and lower limits are designated with arrows and unfilled markers. The R25 galaxies well match the observations from the COS-Halo Survey; however, we note that they are systematically higher than the upper limits of the more massive ellipticals in the survey. (This is likely due to the high virial temperature of these more massive galaxies ionizing oxygen into higher states such as OVII and OVIII. We discuss this further in the results section.) We further compare the column densities of OVI in the R25 galaxies to the 4 zoom-in galaxies with BH physics and find that these galaxies also well match the observed column densities of COS-Halo and fall within the range of the R25 galaxies (Figure **??**.

To further understand the effects of the AGN in our galaxies, we examine the column densities of OVI in the CGMs of our 4 zoom-in galaxies without BH physics and compare them to the cases where BH physics is included. Figure 6 shows the column densities of OVI in the CGM of all four of our zoom-in galaxies with BH physics (solid lines) and without (dashed lines). We can see that in the cases where BH physics is not included, the value of $N_{OVI}$ are significantly lower implying that the presence of the AGN must play an important role in populating OVI in the CGM. We will discuss the ramifications of this further in the Results section.

## 4. RESULTS

Figure 3 shows the phase diagrams for all 4 of our zoom-in GM galaxies with (*Left column*) and without BH physics (*Right column*). For the galaxies that include BH physics, there is surprisingly little difference between the star forming galaxies (P0 and GM1) and quenched galaxies (GM2 and GM3). Furthermore, fewer distinguishing features appear between the BH physics and no BH cases. In particular, it's interesting to note that the removal of the BH physics in all four zoom-ins causes the final characteristics of the main halo to have very little difference (Table 2). These surprisingly similar phase diagrams, however, are further understood by examining the column densities of OVI in their CGMS.

Figures 4 and 5 make it clear that our galaxies are well-simulating the column densities of OVI in the CGM; however, this conclusion is not the only important feature of these plots. In addition, we note that *the column densities of OVI in the CGMs of these galaxies does not seem to depend on the morphology of the galaxy.* In both the R25 galaxies and the zoom-in galaxies, it doesn't matter whether the resulting galaxy at z = 0 is a spiral galaxy or has been quenched, all of these galaxies within this mass range match well with the COS-Halo observations. It's clear that the CGM does not seem to

*Result 1:* From this study, we determine that morphological evolution of the galaxy doesn't correlate with the evolution of the CGM. Instead, it appears that the mass of the galaxy, and connectedly its virial temperature [Table 1], plays a more significant role in determining the amount of OVI seen in the CGM. (Cite Oppenheimer in Discussion)

In addition to providing evidence for our initial result, the R25 simulation give **cosmological credence** to our suite of GM galaxies. We see the same confirmation of our result within Patient 0 and its GMs, which include two star forming galaxies and four quenched galaxies. (Figure 5) (Also here: We leave the examination of the quenching mechanisms affecting this galaxy and its GMs to a future paper.) As mentioned, the benefits of the individual zoom-in galaxies include the ability to remove or adjust the physical parameters affecting our galaxies to test different theoretical models (which would be too computationally expensive to do with a large volume like R25.)

When we examine the secondary suite of GM simulations (without BH physics), we see a significant change in the amount of OVI present in the CGM. (Figure 6). We examine the temperature, mass, density, and metallicity of the CGM to investigate the cause of this decrease in OVI. (Figure 7)

The difference between the CGMs of these two cases appears to come directly from the change in metallicity due to the lack of black hole activity. (Figure 7) We examine the metallicity of the disk to look for further clues about how the lack of AGN activity is affecting the galaxy. Figure 9 shows that, in the galaxies without BH physics, the metals produced in the disk aren't populated into the CGM due to the lack of AGN feedback. Surprisingly, however, the feedback doesn't seem to play a role in significantly heating or excavating the CGM gas, but it appears the the AGN's feedback is pivotal in transporting the *metals* from the center of the galaxy out into the CGM. *The AGN plays a significant role in physically driving the metals out of the disk and into the outer regions of the CGM.*

We further examine the effects of the BH by looking to the mass buildup and accretion rate of the BHs. (Figure 8)

## 5. DISCUSSION

**Result 1: OVI as a Tracer for Virial Temperature of the Halo**

The combined, consistent results of the cosmologi-

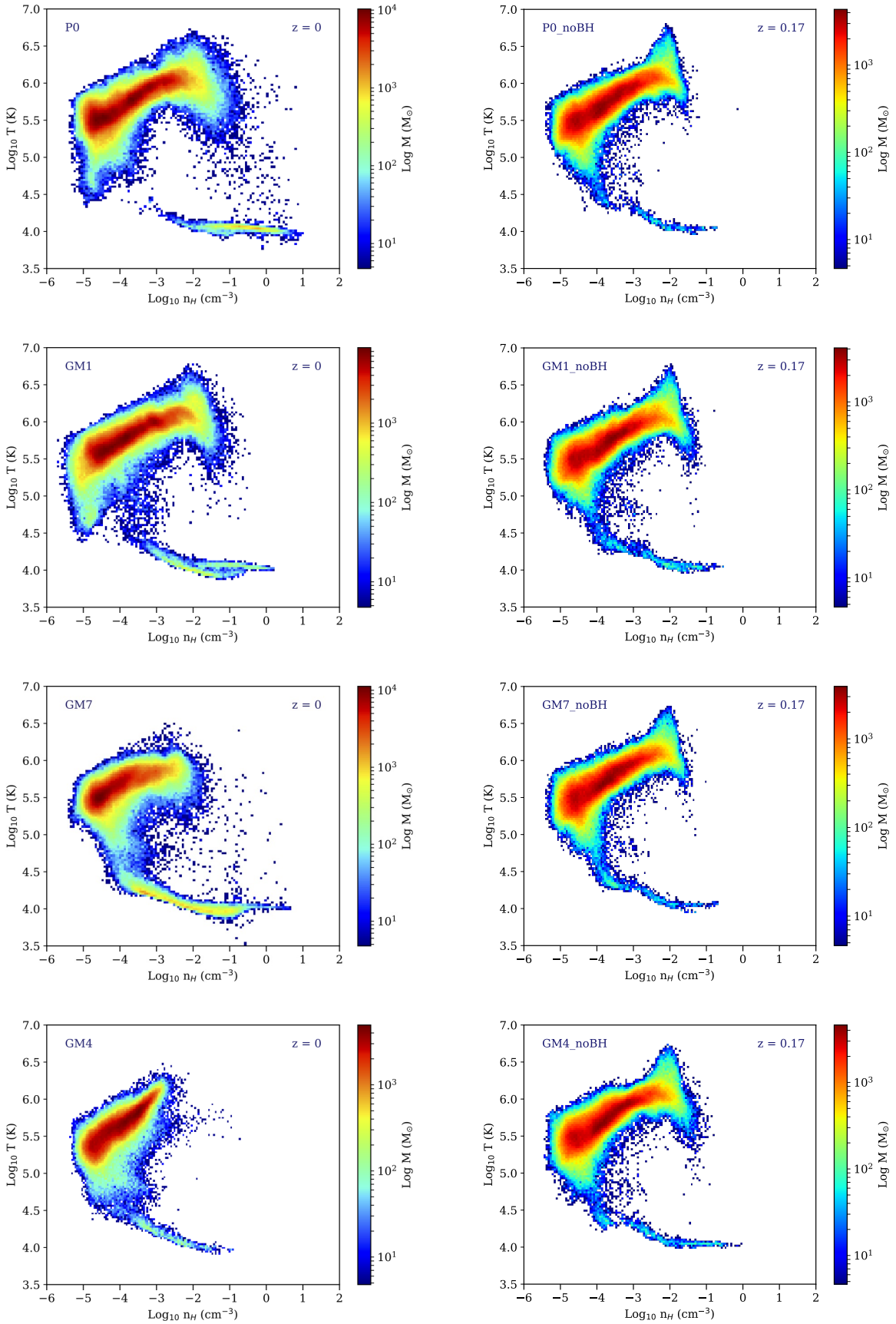


FIG. 3.— Phase diagrams of the temperature and density of the two star forming zoom-in galaxies, P0 (*Top row*) and GM1 (*Second row*), and the two quenched galaxies, GM2 (*Third row*) and GM3 (*Bottom row*). The galaxies .

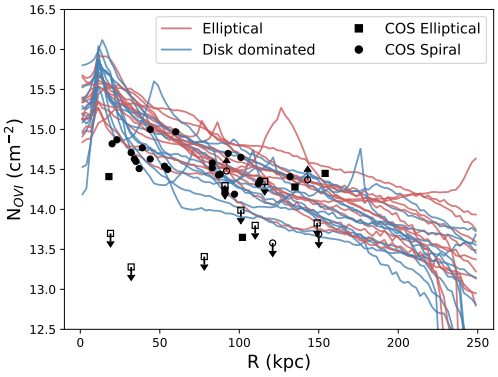


FIG. 4.— Column densities of OVI as a function of radius for all Milky Way mass halos in the R25 simulation. Blue and red lines distinguish between disk dominated spirals and quenched elliptical galaxies within the R25 simulation. Black filled circles and squares indicate spirals and ellipticals from the COS-Halo Survey dataset. Unfilled circles and squares indicate upper and lower limits.

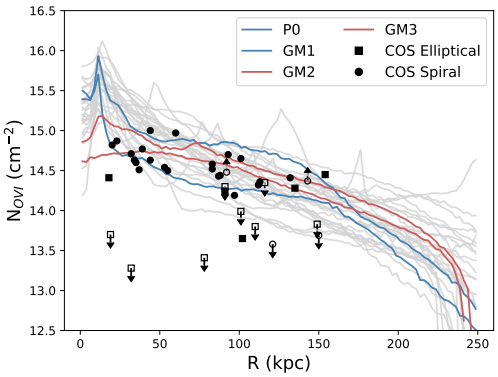


FIG. 5.— Column density profiles of OVI in our 26 R25 and 4 zoom-in GM galaxies. Grey lines are as in Figure 4, and describe our 26 MW-mass R25 galaxies. Blue solid lines describe our two star forming galaxies, P0 and GM1. GM4-7, our passive galaxies, are in solid red. Black circles indicate

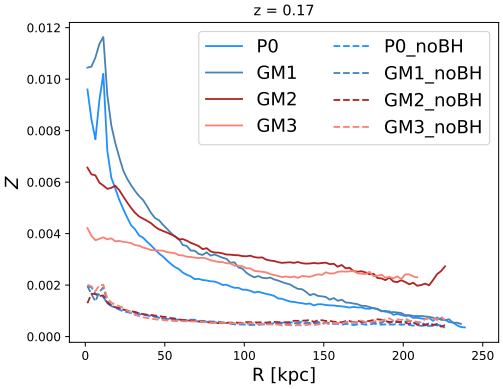


FIG. 6.— Column density profiles of OVI in our 4 zoom-in galaxies with (solid lines) and without (dashed lines) BH physics. P0 and GM1, our two star forming galaxies are colored as light blue and dark blue, respectively. Our quenched galaxies, GM2 and GM3, are labeled in dark red and pink, respectively.

cal R25 and our 4 zoom-in galaxies (which include BH physics) imply a mechanism by which column densities of OVI are optimized by the virial temperature of the CGMs host galaxy, rather than any affect by the evolution of a disk. Their phase diagrams also lack significant difference in their overall morphology, except where more gas is clearly present in the higher mass galaxies. Therefore, we surmise that the difference in the CGM are less motivated by the quenching of a galaxy but rather these differences are primarily driven by the virial temperature of the galaxy.

These results are consistent with Oppenheimer et. al. 2016 who used a suite of EAGLE simulated galaxies and found the bimodality of OVI column densities (further discussed in [Tumlinson 2011]) in star forming and quenched galaxies. They argue that the star forming galaxies ($10^{11}$ - $10^{12}$), which were found to have a higher fraction of OVI, were at the right virial temperature to maximize OVI production, while their quenched galaxies ($10^{12}$ - $10^{13}$) had high enough virial temperatures such that the dominant ionization state was not OVI but rather OVII or above. Oppenheimer et. al. 2016 argues that the OVI content was not a tracer of star formation directly, but rather a more direct thermometer for the temperature of the halo.

We note that the quenched galaxies in our sample are smaller in mass than our star forming galaxies, unlike those in Oppenheimer, explaining the lack of bimodality that we observe. While all the GMs are in the mass range to have virial temperatures which optimize OVI, we further examine the R25 simulation's higher mass, passive galaxies to see if the bimodality appears. (Figure

Furthermore, examining galaxies with masses larger than our MW-mass GMs ($>2 \times 10^{12}$) from the R25 suite, we see that the column densities of OVI decrease as the ionization peak of OVI is surpassed by these halos. Since the virial temperature is higher, the oxygen is likely to be ionized to a higher ionizations state (OVII or OVII), which we show is the case in Figure 10. **NEED TO INCLUDE OVII PLOT**

**Result 2: AGN as driver for metals in the CGM**

Our result that the AGN acts a physical driver for metals in the CGM has interesting consequences. Previous studies have examined the effect of heating on the CGM as the AGNs energy input may put the gas into phases which optimize the production of OVI. (Suresh et al. 2017) Others have proposed that the feedback from AGN may physically drive outflows of gas out of the galaxy, resulting in a lower density CGM and therefore lower densities of OVI. Neither of these cases are what we see. *Instead, we see a suite of CGM which rely on the AGN for the propagation of metal mass (but not total gas mass) into the outer galaxy and OVI columns which depend on the virial temperature of the galaxy.*

## 6. CONCLUSION

Acknowledge some cool peeps.

## REFERENCES

Governato, F., Weisz, D., Pontzen, A., et al. 2015, Monthly Notices of the Royal Astronomical Society, 448, 792 2.1

Haardt, F., & Madau, P. 2012, The Astrophysical Journal, 746, 125 2.1

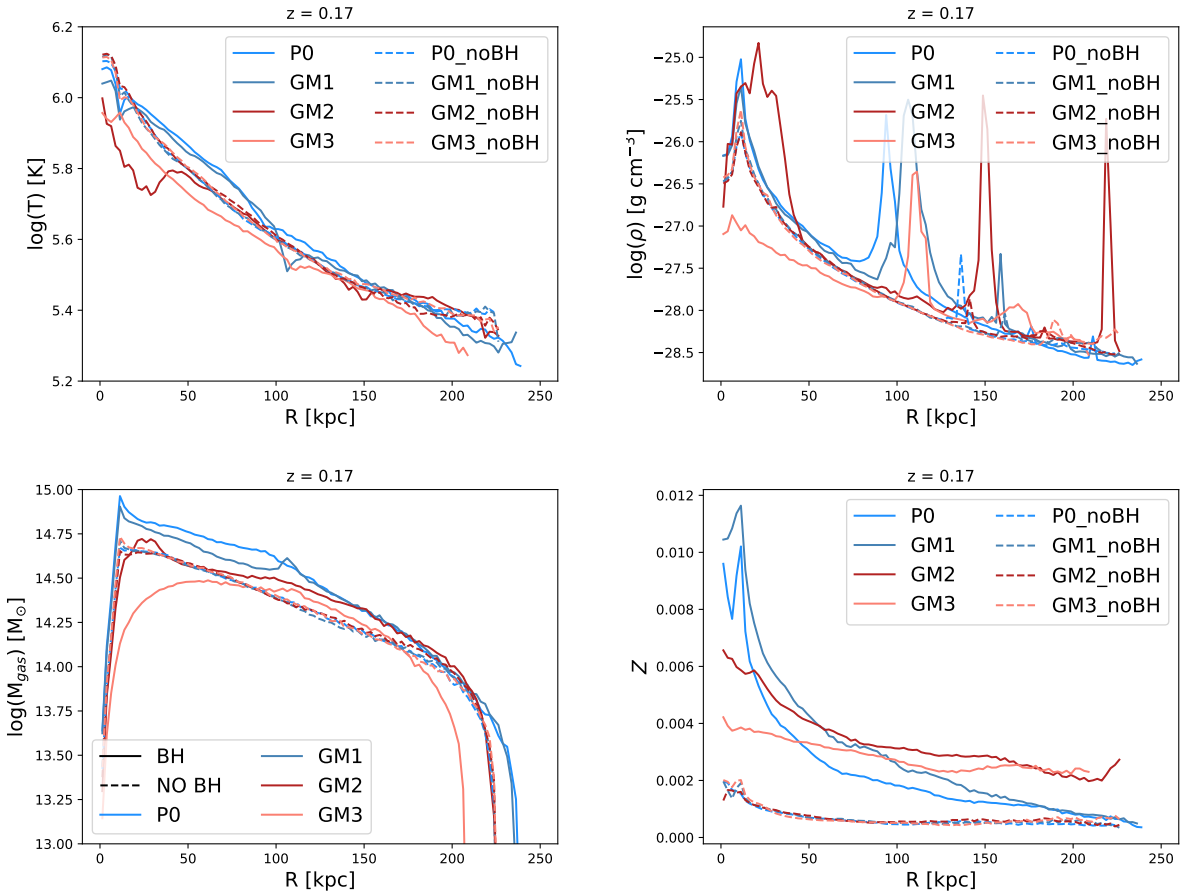


FIG. 7.— Temperature, Total Mass, Total Density, and Metallicity profiles of the CGM of our 4 zoom-in galaxies with and without BH physics. Colors and linestyles as in Figure 6.


Knollmann, S. R., & Knebe, A. 2009, The Astrophysical Journal Supplement Series, 182, 608 3

Menon, H., Wesolowski, L., Zheng, G., et al. 2015, Computational Astrophysics and Cosmology, 2, 1 2.1

Oppenheimer, B. D., Crain, R. A., Schaye, J., et al. 2016, Monthly Notices of the Royal Astronomical Society, 460, 2157 10

Pontzen, A., Tremmel, M., Roth, N., et al. 2017, Monthly Notices of the Royal Astronomical Society, 465, 547 1, 2.3

Ritchie, B. W., & Thomas, P. A. 2001, Monthly Notices of the Royal Astronomical Society, 323, 743 2.1

Roth, N., Pontzen, A., & Peiris, H. V. 2016, Monthly Notices of the Royal Astronomical Society, 455, 974 1

Shen, S., Wadsley, J., & Stinson, G. 2010, Monthly Notices of the Royal Astronomical Society, 407, 1581 2.1

Stinson, G., Seth, A., Katz, N., et al. 2006, Monthly Notices of the Royal Astronomical Society, 373, 1074 2.1

Suresh, J., Rubin, K. H. R., Kannan, R., et al. 2017, Monthly Notices of the Royal Astronomical Society, 465, 2966 5

Tremmel, M., Governato, F., Volonteri, M., & Quinn, T. R. 2015, Monthly Notices of the Royal Astronomical Society, 451, 1868 1, 2.1, 2.3

Tremmel, M., Karcher, M., Governato, F., et al. 2017, Monthly Notices of the Royal Astronomical Society, 470, 1121 1, 2.1, 2.2

Wadsley, J., Stadel, J., & Quinn, T. 2004, New Astronomy, 9, 137 2.1

Wadsley, J. W., Veeravalli, G., & Couchman, H. M. P. 2008, Monthly Notices of the Royal Astronomical Society, 387, 427 2.1

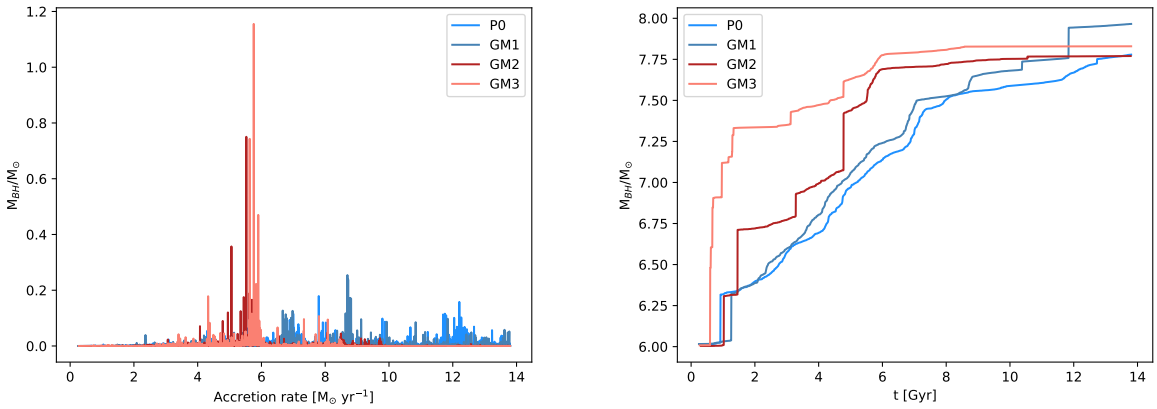


FIG. 8.— BH accretion rates (*Left*) and BH mass (*Right*) for our 4 zoom-in galaxies. Colors as in Figure 6.

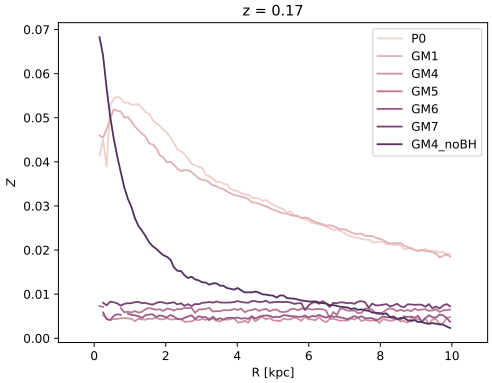


FIG. 9.— [Fix colors] Metallicity profile of the gas within the disk of our 12 GM galaxies. Colors and line styles as in Figure . Without the black hole physics, metals remain trapped near the center of the disk with no mechanism to propagate out into the CGM

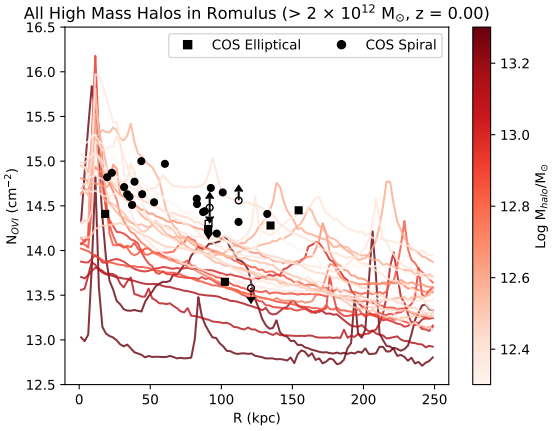


FIG. 10.— Profiles of the column densities of OVI for High Mass galaxies in the R25 simulation. The color bar describes total mass of the halo within the virial radius. As describes in Oppenheimer et al. (2016), NOVI values are lower for more massive, passive galaxies due to the higher virial temperatures they reach which ionize oxygen to higher states, such as OVII.